ARTICLES

Analysis of Intermolecular Coordinate Contributions to Third-Order Ultrafast Spectroscopy of Liquids in the Harmonic Oscillator Limit

Dale McMorrow,* Napoleon Thantu,† Valeria Kleiman,‡ and Joseph S. Melinger

Naval Research Laboratory, Code 6820, Washington, D.C. 20375

William T. Lotshaw*

General Electric Research and Development Center, P.O. Box 8, Schenectady, New York 12301

Received: July 7, 2000; In Final Form: May 2, 2001

The apparently-multicomponent subpicosecond intermolecular dynamics of carbon disulfide liquid are addressed in a unified manner in terms of an inhomogeneously broadened quantum mechanical harmonic oscillator model for a single vibrational coordinate. For an inhomogeneously broadened (Gaussian) distribution of oscillators, the model predicts naturally the bimodal character of the subpicosecond intermolecular dynamics of carbon disulfide liquid, and also the spectral evolution effects (spectral narrowing and saturation) that are observed for solutions of carbon disulfide in weakly interacting alkane solvents. The unique dynamical signature of these low-frequency vibrational coordinates is determined largely by the physical constraints on the coordinates (near equality of oscillator frequency, dephasing frequency, and inhomogeneous bandwidth), such that constructive and destructive interference effects play a dominant role in shaping the experimental observable.

I. Introduction

The microscopic origins of the unique spectral and dynamical characteristics of the intermolecular degrees of freedom in liquids have been the subject of inquiry for more than three decades.[1−54] Recent advances in nonlinear-optical spectroscopy[13,16,18−20,32,36,38,43] and theoretical approaches[37,45−54] have added significantly to our recognition and understanding of these dynamic coordinates and led to a resurgence of interest in this area. Despite these advances, a satisfactory understanding of intermolecular structure and dynamics of liquids remains elusive.

The primary objective of this report is to present a model that accounts for the apparently universal signature of the subpicosecond nonlinear-optical (NLO) response of molecular liquids.[16,17,21−23,29−31,55−59] This characteristic signature is illustrated in Figure 1, which shows the nondiffusive nuclear contributions to the optical Kerr effect (OKE) impulse response function of neat CS_2 and a 10% (by volume) solution of CS_2 in isopentane. The response consists of an inertially delayed (∼150 fs) rise, an initially rapid, Gaussian-like decay, followed by a slower, approximately exponential relaxation. Also apparent in the neat CS_2 data is evidence for a weak oscillation with a period of approximately 800 fs.[74] Details of the data analysis procedures used to extract these response functions are given below.

This unique temporal signature was initially observed in the OKE responses of nitrobenzene and chlorobenzene liquids;[55] carbon disulfide, chloroform, and methylene chloride;[16] and numerous other liquids shortly thereafter.[23,56−61] We believe that the functional form of this response reflects a universal property of low-frequency intermolecular motions in liquids,[27,59] and that a mechanistic understanding of the origin of this characteristic temporal signature will improve our understanding of molecular motion in liquids in general, and the nature of nondiffusive intermolecular degrees of freedom in liquids in particular.

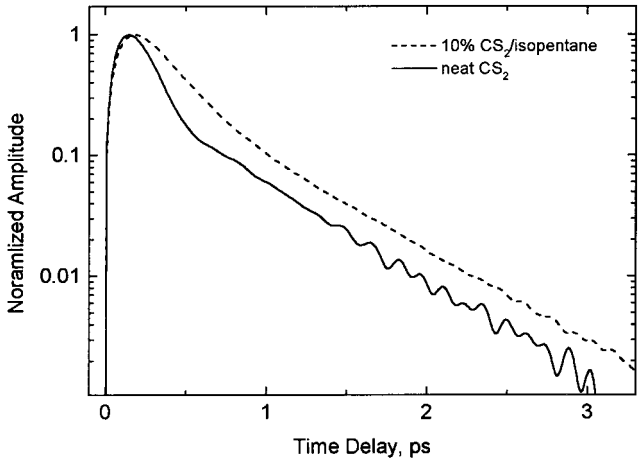

Figure 1. Nondiffusive (vibrational) nuclear contributions to the OHD OKE impulse response function of *neat* CS_2 (solid line) and a 10% (by volume) solution of CS_2 in isopentane (dashed line).

The most elementary interpretations of the universal temporal signature of molecular liquids are based on multimode curve

† Current address: Idaho National Engineering and Environmental Laboratory, MS 2211, P.O. Box 1625, Idaho Falls, ID 83415.

‡ SFA, Inc., Landover, MD; under contract to NRL; current address: Department of Chemistry, University of Florida, Gainesville, FL 32611

10.1021/jp002449k CCC: $20.00
Published on Web 07/27/2001

fitting analyses.[16,17,21,22,27−29,61] Although these are straightforward to implement, and have provided significant physical insight, the assignment of the different fitted components to unique intermolecular degrees of freedom is not justified in general. The first attempt to address the unique characteristics of the intermolecular dynamics in a self-consistent fashion utilized an inhomogeneously broadened classical-mechanical harmonic oscillator (HO) model for the intermolecular coordinates.[27,59] The recognition that the oscillator damping/dephasing mechanisms in liquids are of the same physical origin, and exhibit a similar frequency dependence, as the motions of the intermolecular coordinates themselves led to a model for the intermolecular coordinates consisting of a superposition of underdamped, critically damped, and overdamped oscillators. That superposition model offered a physically intuitive account for the qualitative characteristics of the experimental data:[27,59] destructive interference of the underdamped oscillators gives rise to the rapid Gaussian-like relaxation, whereas constructive interference of the critically damped and overdamped oscillators results in the slowly relaxing tail. As described below, however, the classical HO model exhibits a serious flaw for continuous distributions of oscillators with nonnegligible amplitudes as $\omega \rightarrow 0$, which is generally the case of interest for intermolecular degrees of freedom in liquids.

In this paper, we revisit the intermolecular dynamics of CS_2 in solutions with weakly interacting alkane solvents. The subpicosecond molecular dynamics of CS_2, as a pure substance and in solution, have been investigated by several laboratories in recent years using diverse (third and higher order) nonlinear-optical techniques.[13,15−17,19,20,27,30−36,38,39,59,61,62] Our initial investigation of CS_2/alkane solutions,[17] which utilized a time-domain multimode curve fitting data analysis, provided significant insight into the role of microscopic interactions in shaping the ultrafast intermolecular dynamics. The conclusions of that work were largely reinforced in a more recent study that utilized Fourier transform/deconvolution data analysis procedures to separate uniquely the nuclear and electronic contributions to the OKE data and generate a spectral density representation of the nuclear dynamics.[27,62] In that study, the interpretation of the intermolecular vibrational contributions to the spectral density was premised on the classical HO model, with the distribution of damping conditions noted above.

Recently, the OKE dynamics of the CS_2/alkane system were analyzed in terms of a multimode Brownian oscillator model.[31] There are few practical distinctions between the Brownian oscillator model and the classical HO representation, and although the physical trends identified in our earlier studies[17,27,62] were largely corroborated, the authors presented some interesting heuristic arguments that led them to question interpretations derived from the multimode and classical harmonic oscillator model analyses. These issues are addressed in the following sections. Another recent report showed a strong correlation between the 1/*e* times for reorientational diffusion and the exponential "tail" of the subpicosecond intermolecular response.[30] That correlation led to the suggestion that the exponential "tail" is a consequence of spectral diffusion of the intermolecular oscillators arising from fluctuations in the intermolecular potential as molecules reorient.

In what follows, we investigate the implications of an inhomogeneously broadened quantum mechanical harmonic-oscillator model[37] for the description of subpicosecond dynamics in molecular liquids. The conclusions of this analysis are, in many ways, similar to those of the classical HO model, with the observed dynamics determined largely by the physical constraints on the intermolecular coordinates. In particular, in the presence of inhomogeneous broadening, the near equality of the oscillator frequencies and (homogeneous and inhomogeneous) dephasing bandwidths gives rise to constructive and destructive interference effects that are unique to these combinations of parameters, and result in the unique temporal signature characteristic of intermolecular modes in liquids (*cf.*, Figure 1). Also, because the relationship between frequency and damping rate (frequency pulling effect) is absent in the quantum model, the transients are well behaved as $\omega \rightarrow 0$. Finally, we show how the evolution of the intermolecular spectral density of CS_2 in serial alkane dilutions can be described by the dependence of a single generalized intermolecular coordinate on multipolar intermolecular interactions.

II. Experimental Section

A. Experimental Details. The experimental procedures of the optical heterodyne detected (OHD) OKE have been discussed previously;[16,26,27,58] only the essential features will be repeated here. The data used in this study were generated using modelocked Ti:sapphire lasers that generate 20−40 fs nearly transform-limited optical pulses near 800 nm. The laser output is divided by an uncoated glass optical flat (BK-7A or fused silica) with the front surface reflection directed through a computer-controlled optical delay line. This probe beam is polarized with a calcite Glan-Taylor polarizer, passed through a broadband $\lambda/4$ waveplate, and focused into the 1 mm fused silica sample cell by a 6 cm focal length achromatic doublet. The probe beam is then recollimated and analyzed by a second matched polarizer, the transmission of which is detected with a photomultiplier tube/lock-in amplifier combination. The signal is recorded as a function of the delay between the pump and probe pulses and stored on a computer.

Static strain birefringence in the lens and sample cell are compensated for by fine adjustments of the waveplate (a corresponding adjustment of the probe analyzer polarizer is sometimes required). The pump beam is polarized 45° relative to the probe with a $\lambda/2$ waveplate/polarizer combination, modulated with a kilohertz chopper, passed through a matched optical flat to balance the arms of the interferometer, and overlapped with the probe beam in the sample by the achromat. The optical local oscillator is introduced with the $\lambda/4$ waveplate positioned between the crossed polarizers oriented with its "fast" axis parallel to the polarization plane of the probe beam. A slight rotation ($<1°$) of the input polarizer introduces a small orthogonal polarization component (the local oscillator) that is 90° out-of-phase with the probe field. The out-of-phase local oscillator is in quadrature with the real part of the nonlinear susceptibility, and the detected (heterodyne) signal (the induced birefringence) is nominally linear in the pump beam intensity.

The heterodyne signal is contaminated with the homodyne signal (which scales quadratically with the pump intensity), with the degree of contamination depending on the amplitude of the local oscillator. The pure heterodyne responses can be recovered by constructing the sum of data scans collected with positively and negatively sensed local oscillators; this operation eliminates the homodyne contamination of the heterodyne signal.[26]

B. Data Analysis Procedures. The theoretical development associated with the optical heterodyne detected optical Kerr effect experiment and the relevant Fourier transform relationships are described in detail elsewhere;[18,58] only the essential expressions will be repeated here. For Fourier transform-limited optical pulses and a local oscillator that is 90° out-of-phase with

the probe field, the transmission function for the Kerr cell is described by the relation

$$T(\tau) = \int_{-\infty}^{\infty} G_0^{(2)}(\tau - t)\, Re\, \chi_{\text{eff}}^{(3)}(t)\, dt = G_0^{(2)}(\tau) * R_{\text{eff}}^{(3)}(\tau) \qquad (1)$$

where $G_0^{(2)}(\tau)$ is the background-free laser pulse intensity autocorrelation function, $R_{\text{eff}}^{(3)}(t) \propto Re\, \chi_{\text{eff}}^{(3)}(t)$ is the time-domain OKE impulse response function of the medium, τ is the delay between pump and probe pulses, and the asterisk (*) indicates a convolution operation. Fourier transformation of 1 gives rise to the frequency-domain product

$$\mathcal{F}\{T(\tau)\} = \mathcal{F}\{G_0^{(2)}(\tau)\}\mathcal{F}\{R_{\text{eff}}^{(3)}(\tau)\} \qquad (2)$$

where the $\mathcal{F}\{\}$ indicate Fourier transform operations. Equation 2 explicitly describes the spectral-filter effect of finite bandwidth optical pulses on the intrinsic frequency response of a material. Because both $T(\tau)$ and $G_0^{(2)}(\tau)$ are experimentally measured functions, the frequency dependent susceptibility can be deduced from 2 using the relationship

$$\chi_{\text{eff}}^{(3)}(\Delta\omega) = \xi \mathcal{F}\{R_{\text{eff}}^{(3)}(t)\} \qquad (3)$$

where $\Delta\omega = \omega_m \pm \omega_n$, the $\omega_{m,n}$ are Fourier components of the pump pulse, ξ is a constant, and $\chi_{\text{eff}}^{(3)}(\Delta\omega)$ is the third-order OKE frequency response function (spectral density) of the material.

In this study, our primary interest is in the nuclear part of the NLO response. The nuclear and electronic contributions can be separated on the basis of symmetry and by recognizing that[18]

$$R_{\text{nuc}}^{(3)}(t) = 2\, \mathcal{F}^{-1}\{Im\, \chi_{\text{eff}}^{(3)}(\Delta\omega)\}\, H(t-t_0) \qquad (4)$$

where $H(t)$ is the Heaviside step function and $R_{\text{nuc}}(t)$ is the nuclear part of the impulse response function. All of the information on the nuclear response of the material to the optical pulses is contained in $Im\, \chi_{\text{eff}}^{(3)}(\Delta\omega)$.[18]

III. Theory

Within the Born−Oppenheimer approximation, the third-order nonlinear-optical impulse response function may be written as a sum of electronic and nuclear parts

$$R_{\text{eff}}^{(3)}(t) = \gamma(t) + R_{\text{nuc}}^{(3)}(t) \qquad (5)$$

In the analysis of experimental data, it is always desirable to describe the dynamics (or spectrum) of a system in terms of a unified model that minimizes the number of free fitting parameters. Unfortunately, the complexity of condensed matter systems often precludes such analyses. In the case of molecular liquids, it is common to treat the nuclear part of the NLO response function as a sum of contributions

$$R_{\text{nuc}}^{(3)}(t) = \sum_i r_i(t) \qquad (6)$$

Equations 5 and 6 form the basis of the commonly used multimode curve-fitting data analyses. In such analyses, functional forms are assumed for a finite number of the r_i, with the various parameters adjusted to obtain the best agreement with the data. For the intermolecular dynamics of highly symmetric species (such as CS_2 and CH_3CN), the experimental OKE data have revealed the existence of three distinct time scales,[16,17,58,59] resulting in a minimum of three terms in eq 6 when the individual r_i are treated as exponential and damped sinusoidal functions.[75] The assignment of the three contributions to specific nuclear coordinates or well-defined physical processes, however, lacks rigorous physical justification.

In what follows, we focus on the nondiffusive contributions to the nuclear dynamics. If we assume separability of the diffusive (orientational anisotropy) and vibrational (nondiffusive) contributions to the signal, the nuclear impulse response function can be represented as a sum of two terms

$$R_{\text{nuc}}^{(3)}(t) = r_v^{(3)} + r_d^{(3)}(t) \qquad (7)$$

Distinguishing between the diffusive and the vibrational contributions as in eq 7 has been widely utilized in the analysis of femtosecond NLO data, and is usually premised on time scale separation arguments.[16,63] For the purposes of this paper, we refer to the "vibrational" part of the signal as those contributions that are nondiffusive in character (e.g., do not conform to Debye−Stokes−Einstein (DSE) type behavior) and typically exhibit subpicosecond decay characteristics. This signal component is associated with dynamically coherent nuclear motions, and can contain contributions from diverse origins such as molecular librational or free rotational motions, translational modes that lead to a net change in the polarizability (through interaction-induced effects), as well as more complex lattice-like "collective" modes that can involve the reorientation and translation of locally ordered groups of molecules. This signal component decays through dephasing and population relaxation. The diffusive contribution, in contrast, is associated with an orientational anisotropy that decays through the random, thermal fluctuations which are highly correlated with bulk properties such as viscosity and diffusivity.

In the following sections, we assume validity of eq 7, and focus our attention on the vibrational nuclear contributions, $r_v^{(3)}(t)$. The experimental data are analyzed in terms of two models that treat the vibrational dynamics in a self-consistent manner. The first is the classical-mechanical HO model noted above;[59] the second is a HO model derived from a quantum-mechanical quantum-mechanical development in which dephasing is implemented in the weak coupling limit.[37] Both models account for the coarse qualitative features of the experimental data, but differ significantly in their low-frequency behaviors. We note that neither model should be considered purely "single-particle" in nature. More correctly, each should be considered an "harmonic coordinate" model in which the precise identity (i.e., single molecular vs collective) of the individual oscillators need not be specified. Although it is tempting to assign response functions to the vibrational motion of single-molecule "librators", and such assignments certainly help develop a physical picture of the system, they could just as easily be identified with delocalized "phonon-like" modes. It is likely that reality lies somewhere between these extremes.

A. Classical Oscillator Model. In previous analyses of intermolecular dynamics,[27,59] we introduced a classical oscillator representation that recognized the unique characteristics of intermolecular vibrational coordinates compared to those of the more familiar intramolecular vibrational modes. Those unique characteristics are a consequence of three effects: (i) the vibrational potential is defined by the (mostly nearest neighbor) intermolecular potential (this is in contrast to intramolecular modes where the intermolecular potential appears as a small perturbation); (ii) the vibrational frequencies span the same time scale as the dephasing and relaxation processes for these modes; and (iii) local fluctuations in the intermolecular potential

responsible for the decay processes also give rise to distributions in the oscillator frequencies (inhomogeneous broadening) that persist over the time scale of the fluctuations. These considerations can be expressed by the relation

$$\omega \approx \omega_c \approx \Delta\omega \tag{8}$$

where ω is the oscillator frequency, ω_c is a critical frequency related to the 1/e time for fluctuations of the liquid local structure (which results in dephasing and relaxation of intermolecular vibrational coordinates), and $\Delta\omega$ is the width of the inhomogeneous frequency distribution of the oscillator.

In the classical oscillator model,[27,59] the first equality of 8 forces consideration of the possibility that any of the three solutions to the classical HO equation of motion, underdamped, critically damped, and overdamped, may contribute to the dynamics of the intermolecular coordinate. This is in stark contrast to the case for intramolecular vibrational modes, which are almost always strongly underdamped. Expressed formally these three solutions are given by

$$r_i(\omega_i,t) = \frac{1}{\omega_i}\exp(-\gamma t)\sin(\omega_i t),\ \omega_{oi} > \gamma \tag{9a}$$

$$r_i(\omega_i,t) = t\exp(-\gamma t),\ \omega_{oi} = \gamma \tag{9b}$$

$$r_i(\omega_i,t) = \frac{1}{\omega_i}\exp(-\gamma_i t)\,[1 - exp(-2\omega_i t)],\ \omega_{oi} < \gamma \tag{9c}$$

in which eqs 9a, 9b, and 9c correspond to the underdamped, critically damped, and overdamped solutions, respectively, ω_{oi} is the undamped frequency of the oscillator. The quantities

$$\omega_i = |\omega_{oi}^2 - \gamma^2|^{1/2} \tag{10a}$$

and

$$\gamma_i = \gamma - \omega_i \tag{10b}$$

are the effective frequency and damping rate, respectively. Equations 10 define the mutual "pulling" of the oscillation frequency and damping rate for classical harmonic coordinates. Of the response functions 9, only the first actually oscillates; the other two rise and decay to zero in a monotonic fashion.

The second equality of 8 implies that, when the vibrational coordinate is inhomogeneously broadened, all three solutions can contribute to the response for a single dynamical coordinate. The vibrational response function then can be represented by a superposition of the solutions 9, and can be represented in the general form

$$r_v^{(3)}(t) = \int_0^\infty d\omega\ g(\omega)\ r^{(3)}(\omega, t) \tag{11}$$

in which the amplitudes of the different frequency components are collected in the distribution function, $g(\omega)$, the subscript v denotes that we are considering only the vibrational part of the nuclear response function (*cf.*, eq 7), the integral is over all frequency components of the inhomogeneously broadened ensemble, and we have written eqs 9 in the more compact form

$$r^{(3)}(\omega_i, t) = \frac{1}{\omega_i}\exp(-\gamma_i t)\sin(\omega_i t) \tag{12}$$

which allows for complex frequency arguments. These general results, eqs 11 and 12, are formally identical to those presented elsewhere[31] for the Brownian oscillator representation in the limit of a linear dependence of the polarizability on the nuclear coordinates.

Equations 9−12 illustrate that, when the physical constraints of the system are recognized (eq 8), the classical harmonic oscillator treatment leads naturally to a superposition of underdamped, critically damped, and overdamped oscillators (a situation that appears to be unique to low-frequency intermolecular degrees of freedom), and this simple functional form can account for the rather complex bimodal dynamical profiles and line shapes of the intermolecular degrees of freedom in a self-consistent manner. Equations 9 through 12 represent the vibrational response of a single intermolecular coordinate. In the event that multiple coordinates contribute to the system response, a superposition of solutions 11 is required.

We point out one obvious shortcoming of the classical model that has not been noted previously. For fixed γ, as the frequency ω_{oi} decreases toward zero, the effective decay rate of an overdamped oscillator, γ_i, also approaches zero (eqs 10). That is, the decay time ($1/\gamma_i$) of an overdamped contribution to the signal increases as the frequency is decreased. This is a general characteristic of classical overdamped oscillators with practical consequences for continuous distributions of oscillator frequencies with nonvanishing amplitude as $\omega \rightarrow 0$ (the common situation for simple molecular liquids). In this case, the classical oscillator model predicts a slowly decaying component in the response function due to the lowest frequency (overdamped) oscillators in the distribution, a result that conflicts with experimental observations (*vide infra*).

B. Quantum Oscillator Model. A quantum mechanical harmonic oscillator representation of the nonlinear-optical response of transparent liquids to electronically nonresonant radiation has been developed in the Born−Oppenheimer limit by Steffen, Fourkas, and Duppen.[37] Response functions for third- and fifth-order NLO processes were characterized in the limits of homogeneous and inhomogeneous broadening of the nuclear transitions. Here, we summarize the key results of that work that are relevant to the third-order processes.

Using a perturbative treatment the nonlinear-optical polarization, third-order in the applied field, may be written in the form[65]

$$P_i^{(3)}(t) = \int_{-\infty}^{\infty} dt_1 \int_{-\infty}^{\infty} dt_2 \int_{-\infty}^{\infty} dt_3\ R_{ijkl}^{(3)}(t,t_1,t_2,t_3), E_j(t_1)E_k(t_2)E_l(t_3) \tag{13}$$

where $R_{ijkl}^{(3)}$ is the third-order nonlinear-optical impulse response function. For transparent media in which all applied optical frequencies are well below any electronic resonances, the Born−Oppenheimer (BO) approximation may be employed. Within the BO approximation, when the optical frequencies are well above all (dipole allowed) nuclear resonances, only two terms contribute to the third-order NLO response function[37]

$$R_{ijkl}^{(3)}(t,t_1,t_2,t_3) = \langle\gamma_{ijkl}\rangle\delta(\tau_1) + \frac{i}{\hbar}\left\langle\left[\tilde{\alpha}_{ij}(t), \frac{1}{2}\tilde{\alpha}_{kl}(t_2)\right]\right\rangle H(\tau_1) \tag{14}$$

The first term on the rhs of eq 14 corresponds to the instantaneous nonlinear electronic hyperpolarizability, and the second term to Rayleigh/Raman scattering processes. In this expression $[A,B]$ denotes a commutator, $\tilde{A}(t)$ indicates that the operator A is in the interaction representation, $\delta(t)$ represents the Kronecker delta function, $H(\tau_1)$ represents the Heaviside step function, and the response function in terms of the (single) positive propagation time, $\tau_1 = t_1 - t_2$ with $t = t_1$ and $t_2 = t_3$, where τ_1 is the delay between the pump and probe laser pulses.[37]

The representation of eq 14 permits identification of the $R^{(3)}_{nuc}(t)$ defined in eq 5 with the commutator of the effective molecular polarizability (for the OKE, the commutator would be over the anisotropic part of the polarizability). We will show later that the subsequent decomposition of $R^{(3)}_{nuc}(t)$ to a sum of linear terms (eq 6) presumes that the polarizability is a strictly linear function of the nuclear coordinates of the medium (the Placzek approximation). The meaning of the quantity $\chi^{(3)}_{eff}(\Delta\omega)$ (eqs 3 and 4) and the linear decomposition of $R^{(3)}_{nuc}(t)$ with respect to the coordinate dependence of the polarizability are discussed in greater detail in section IV-E.

An expression for the third-order polarization may be found by inserting eq 14 into eq 13. A more useful expression for the response function is obtained by evaluating the commutators and transforming the polarizability operators back into the Schrödinger representation[37]

$$\langle\lambda|\tilde{\alpha}(t)|\mu\rangle = \langle\lambda|\alpha|\mu\rangle\, e^{i(\epsilon_\lambda - \epsilon_\mu)t/\hbar} \equiv \alpha_{\lambda\mu} e^{i\omega_{\lambda\mu}t} \qquad (15)$$

giving the result

$$R^{(3)}(\tau_1) = \langle\gamma\rangle\delta(\tau_1) + \frac{1}{\hbar}\sum_{\lambda,\mu} P(\lambda)\, \alpha_{\lambda\mu}(q)\, \alpha_{\mu\lambda}(q)\, \sin(\omega_{\lambda\mu}\tau_1) \qquad (16)$$

where $P(\lambda)$ denotes the equilibrium distribution of eigenstates $|\lambda\rangle$, ϵ_λ is the energy of eigenstate $|\lambda\rangle$, the dependence of the polarizability on the nuclear coordinates "q" is explicitly indicated, and for simplicity, the tensorial notation has been suppressed. Again, because we are interested only in the nuclear response functions, from this point forward we consider only the second term on the rhs of 16.

The response function 16 is a general result for nuclear motion under nonresonant excitation, and does not depend on the specific forms of the Hamiltonian or the polarizability operator.[37] Calculation of the matrix elements $\alpha_{\lambda\mu}$ requires the adoption of a model for nuclear motion. For harmonic motion, the nonlinear-optical response function can be transformed into terms of the HO eigenstates $|\lambda\rangle$. Under the constraints of damping in the weak coupling limit and a linear dependence of the polarizability on nuclear coordinates, the quantum HO expression for the third-order nonlinear response function becomes[37]

$$r^{(3)}_{\upsilon}(\tau_1) = -\frac{\alpha_1^2}{2m\omega} sin(\omega\tau_1)\sum_{\lambda} P(\lambda)[\lambda e^{-\Gamma_{\lambda,\lambda-1}\tau_1} - (\lambda+1)e^{-\Gamma_{\lambda,\lambda+1}\tau_1}] \qquad (17)$$

where α_1 is defined by the polynomial expansion $\alpha(q) = \alpha_1 q + \alpha_2 q^2 + \cdots$, and the subscript υ indicates that we consider only the nuclear (vibrational) contribution to eq 16. When damping is assumed to be independent of the quantum number (level independent damping) eq 17 reduces to

$$r^{(3)}_{\upsilon}(\omega,t) = \frac{\alpha_1^2}{2m\omega} e^{-\Gamma t}\, sin(\omega t) \qquad (18)$$

in which the dephasing is fully described by a single decay rate of the form

$$\Gamma = \gamma + \Gamma^* \qquad (19)$$

In this expression, γ is the population decay rate, Γ^* is the pure dephasing rate and, for the present analysis, we assume that Γ is frequency independent. Inhomogeneous broadening is considered using eq 11 in the same manner as for the classical oscillator model.

Equation 18 is similar to eq 12, with one notable exception; in the weak coupling, limit the frequency and damping arguments of eq 18 are not constrained by the frequency pulling relationships of eqs 10. Thus, the oscillators described by 18 are, in the classical sense, always underdamped, and approach the critically damped limit (eq 9b) when $\Gamma > \omega$. For an inhomogeneously broadened ensemble of molecular oscillators (eq 11), the practical consequences of the quantum oscillator model (eq 18) are similar to those of the classical model (eqs 9, 10, and 12): destructive interference of the more strongly underdamped components gives rise to a rapid, Gaussian-like decay, followed by a quasi-exponential relaxation arising from constructive interference of the nearly critically damped components. The key distinction being that, for the weak coupling model, *the absence of overdamped oscillators ensures that the ensemble-averaged dynamical profile decays in a physically realistic manner* at longer times, a result that gives rise to excellent agreement with the experimental data.

IV. Results and Discussion

In what follows, we analyze the experimental OHD OKE data for *neat* CS_2 and its solutions in alkane solvents in terms of the classical and quantum harmonic oscillator models presented above. It is shown that, although the classical model diverges significantly from the experimental data at long times ($\tau > 1.5$ ps), the quantum-mechanical model does an excellent job of describing the CS_2 data at all times. In particular, the "universal" response of the low-frequency intermolecular modes: a Gaussian-like initial decay followed by a quasi-exponential, intermediate time scale relaxation, is correctly predicted by the response function for a *single* inhomogeneously broadened nuclear coordinate. Further, we find that for a Gaussian distribution of oscillator frequencies, the quantum-based model describes the dynamical and spectral evolution observed on increasing dilution in alkane solvents, and accounts naturally for the experimentally observed[31,27] saturation of the spectral shift at low CS_2 concentrations.

A. Intermolecular Vibrational Dynamics of CS_2. The essential details of the third-order NLO response of CS_2 can be seen in the data of Figure 1, which shows the intermolecular vibrational part of the OHD OKE impulse response functions for *neat* CS_2 and a 10% solution of CS_2 in isopentane. The impulse response functions of Figure 1 were generated from the measured OKE data using eqs 2−4, with the tail-matched diffusive reorientational contribution removed in accordance with eq 7. Analogous results are obtained for the other alkane solvents investigated.[27]

These data reveal clearly the ubiquitous signature of intermolecular dynamics in liquids: inertially delayed rise and a bimodal decay consisting of a rapid Gaussian part followed by a slower quasi-exponential relaxation. On dilution in alkane solvents, the response function evolves toward a more exponential decay characteristic, with the relative amplitude of the Gaussian-like contribution decreased (cf., Figure 1). This evolution is most apparent in a spectral density representation of the data (cf., eq 4), where the vibrational spectrum changes shape significantly as it narrows and shifts to lower frequency with increasing dilution. Examples of this spectral evolution are given in references 27 and 31.

A description of the CS_2/alkane OKE data in terms of an inhomogeneously broadened ensemble of intermolecular harmonic oscillators leads naturally to an intuitive physical picture

that describes the observed spectral evolution. Within this framework, the curvature of the multipole intermolecular potential is decreased as the CS_2 molecules are replaced in the liquid by the weakly interacting alkane species, giving rise to a shift of the spectral density to lower frequencies.[17,27] In the discussion below, it is shown that, within the quantum harmonic oscillator model, the number density effect on the intermolecular potential is the dominant factor contributing to the spectral evolution observed for the CS_2/alkane system, and that (higher-order) interaction-induced effects, which have been shown by simulations to make a small contribution the intermolecular spectral density,[52] need not be implicated.[31]

The two HO models described in section III can be applied to inhomogeneously broadened systems through the use of eq 11. This requires the choice of a distribution function, $g(\omega)$. Assuming that the inhomogeneity is a consequence of a Gaussian random process, a Gaussian form for $g(\omega)$ might be expected. Two Gaussian functions that meet the boundary conditions for intermolecular vibrational modes have been used to represent $g(\omega)$. The first is the "antisymmetrized" Gaussian function[61]

$$g(\omega) = \frac{1}{2\sigma}\left\{\exp\left[-\frac{(\omega-\omega_o)^2}{2\sigma^2}\right] - \exp\left[-\frac{(\omega+\omega_o)^2}{2\sigma^2}\right]\right\} \tag{20}$$

and the second is commonly referred to as the "modified Gaussian" function

$$g'(\omega) = \omega\exp\left[-\frac{(\omega-\omega_o)^2}{2\sigma^2}\right] \tag{21}$$

in which ω_o and σ are parameters which, for an isolated Gaussian distribution, correspond to the center frequency and standard deviation, respectively. In what follows, since the functions of eqs 20 and 21 are not symmetric about ω_o, we refer to ω_o and σ as the characteristic frequency and width parameters, respectively. These two functions are very similar for low-frequency resonances, and parameters can be chosen such that the frequency distributions of the two are nearly identical (although the parameters for each will be different). For the range of parameters relevant to the current analysis, the only significant difference between the two is that the antisymmetrized Gaussian carries somewhat more amplitude on its low-frequency edge when the parameters are adjusted to ensure that the two distributions match at the peak and on the high-frequency edge. In this study, we utilize both functions in analyses of the experimental data for both HO models, with the results being similar for each. We note that the "antisymmetrized" form of the Gaussian function given in eq 20 arises naturally in the OKE because the spectral density function is antisymmetric about $\Delta\omega = 0$ (it is common practice to plot only the positive-frequency half). In the limit that $\omega_o \gg \sigma$, as is generally true for intramolecular modes, the positive and negative frequency contributions to eq 20 do not interfere and can be treated independently. It is only in the limit that ω_o and σ are of the same magnitude that it is necessary to consider both terms explicitly as in eq 20.

B. Application of the Classical Model. The *neat* CS_2 OHD OKE vibrational impulse response function is shown again in Figure 2, together with a fit to the classical oscillator model described in section IIIA (eq 11 using the response function from eqs 9, 10, and 12). The parameters used in this fit are identical to those of reference 31 and, therefore, the modified

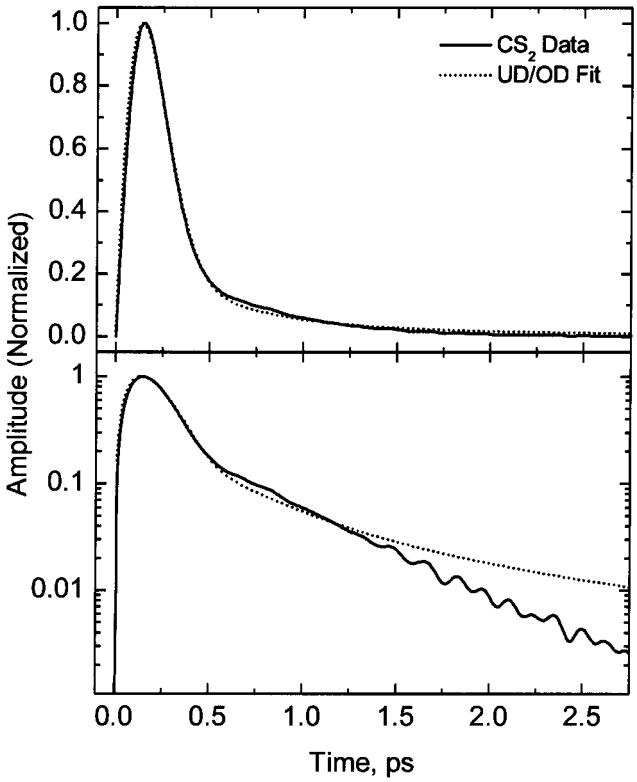

Figure 2. OHD OKE vibrational impulse response function for neat CS_2 (solid line) is shown together with a fit (dashed line) to the classical harmonic-oscillator model. $\omega_o = 7.08$ ps^{-1}; $\sigma = 2.77$ ps^{-1}; $\gamma = 5.26$ ps^{-1}.

Gaussian model is used in this case. Clearly evident, especially in the log plot, is the divergence of the fit from the data at times greater than 1 ps. This divergence is a consequence of the inclusion of overdamped oscillators in this model response function, and the mutual pulling of the oscillator damping and frequency (eqs 10), as is discussed in section IIIA above, and is a general result for distribution functions $g(\omega)$ that have any significant amplitude for frequencies below the critical frequency of $\omega_{oi} = \gamma$. Similar results are obtained for the antisymmetrized Gaussian function, with the exception that the divergence at long times is somewhat greater. We note that the failure evident in Figure 2 is for the particular classical HO model described in section III. It is entirely possible that other approaches based on classical dynamics, such as the stochastic models of Kubo,[66] may provide an equally adequate description of the experimental data as the quantum-mechanical-based model described below.[76]

C. Application of the Quantum Model. The CS_2 OHD OKE vibrational impulse response function is shown again in Figure 3, this time with a fit to the inhomogeneously broadened quantum oscillator model described in section IIIB (eq 11 using the response function eq 18). Neglecting the normalization factor, the fitting procedure involves three parameters: ω_o and σ of the distribution function (eq 20), and Γ of the oscillator impulse response function (eq 18). Parameters for the fit shown in Figure 3, and those for the pentane dilutions (vide infra), are collected in Table 1.

As is evident, the quantum HO oscillator model for a single nuclear coordinate does an excellent job of describing the temporal dynamics of the *neat* CS_2 OKE vibrational response function at all probe delays. We note that the only adjustable parameters are those cited in the previous paragraph, and that there are no independent parameters for adjusting the relative amplitudes of the Gaussian-like and quasi-exponential features

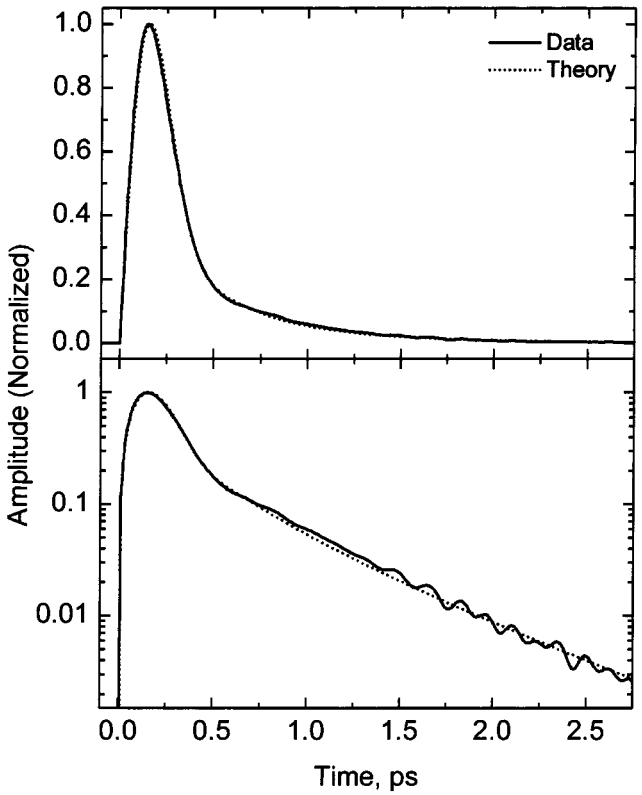

Figure 3. OHD OKE vibrational impulse response function for *neat* CS_2 (solid line) is shown together with a fit (dashed line) to the quantum mechanical harmonic-oscillator model. $\omega_o = 8.5$ ps^{-1}; $\sigma = 5.0$ ps^{-1}; $\gamma = 1.10$ ps^{-1}.

TABLE 1

	ω_o (ps^{-1})	$\bar{\nu}_o$ (cm^{-1})[a]	σ (ps^{-1})	$\bar{\sigma}$ (cm^{-1})[a]	1/Γ (ps)
neat	8.5	45	5.0	27	0.91
75%	7.0	37	6.0	32	0.85
50%	5.5	29	6.0	32	0.91
20%	2.0	11	5.5	29	0.70

[a] $\nu_o = \omega_o/2\pi c$; $\bar{\sigma} = \sigma/2\pi c$.

of the fitted functions. Similar results are obtained when the modified Gaussian distribution function is used with the quantum oscillator model. A significant conclusion from the result of Figure 3, then, is that the quantum oscillator model, which is based solely on a Gaussian distribution of exponentially damped harmonic oscillators, provides a remarkably accurate account for both the qualitative characteristics and the quantitative details of the experimental data.

D. CS_2/Alkane Dilution Data. Figure 4 shows the simulated behavior of the quantum oscillator model under conditions that are similar to those observed for the CS_2/alkane dilutions. This example illustrates the behavior of the inhomogeneous response function (eq 11) using the antisymmetrized Gaussian distribution function (eq 20) as a function of ω_o with σ and Γ held constant. The parameters chosen for the highest-frequency distribution correspond to those extracted from the fit of Figure 2 for *neat* CS_2: $\omega_o = 8.5$ ps^{-1} (45 cm^{-1}), $\sigma = 5.0$ ps^{-1} (26.6 cm^{-1}), and $\Gamma = 1.1$ ps^{-1}.

It is clear from these simulations that, as ω_o is decreased, the temporal response broadens and the Gaussian-like contribution becomes less prominent. For ω_o values below 2.5 ps^{-1} ($\sim$ 13 cm^{-1}), *the dynamical profile undergoes no significant further evolution*. The 2.0 ps^{-1} curve of Figure 4, therefore, represents a limiting case after which no further evolution in the dynamical profile occurs.

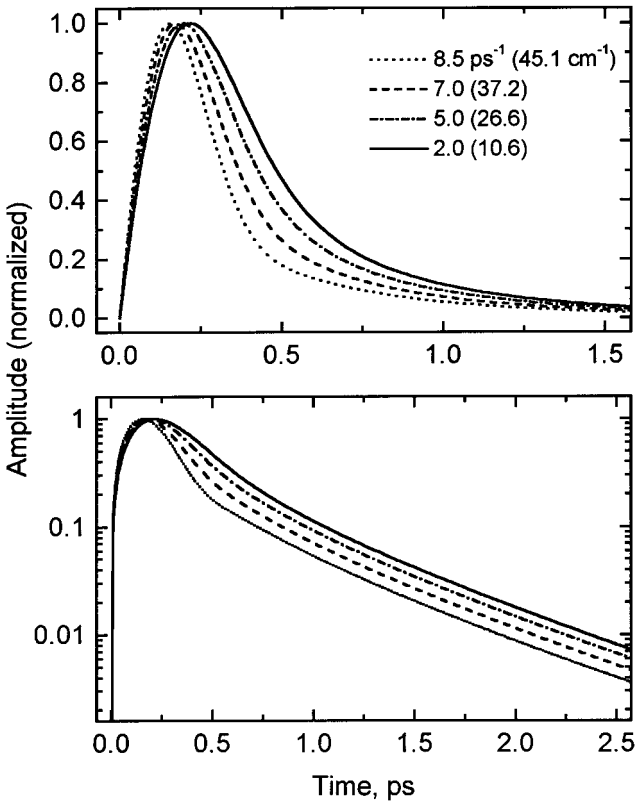

Figure 4. Behavior of eq 11 using the antisymmetrized Gaussian distributionfunction (eq 21) as a function of ω_o with σ and Γ held constant. $\sigma = 5.0$ ps^{-1} (26.6 cm^{-1}), and $\Gamma = 1.1$ ps^{-1}.

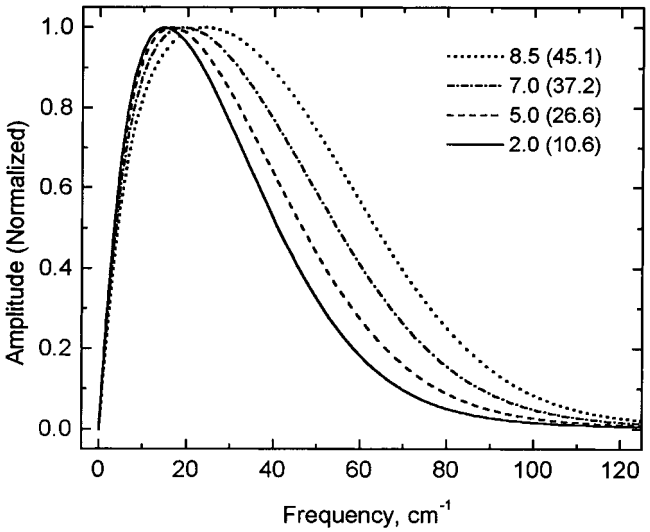

Figure 5. Spectral density representation of the data of Figure 4. The spectral evolution saturates for ω_o values less than 2.5 ps^{-1} (13.3 cm^{-1}), with the 2.0 ps^{-1} curve representative of this limiting case.

A frequency-domain representation of the Figure 4 result is shown in Figure 5. As is evident, the spectral density narrows and shifts to lower frequency as the characteristic frequency of the distribution, ω_o, is reduced. Analogous to the time-domain data, the spectral evolution saturates for ω_o values below 2.5 ps^{-1}, with the 2.0 ps^{-1} curve representing the limiting case. The results of Figures 4 and 5 bear a striking resemblance to the CS_2/alkane OKE data, examples of which are illustrated in Figure 1 and in references 27 and 31.

A significant characteristic of the simulations of Figures 4 and 5 is the saturation of the spectral/dynamical evolution as the characteristic frequency of the oscillator distribution function

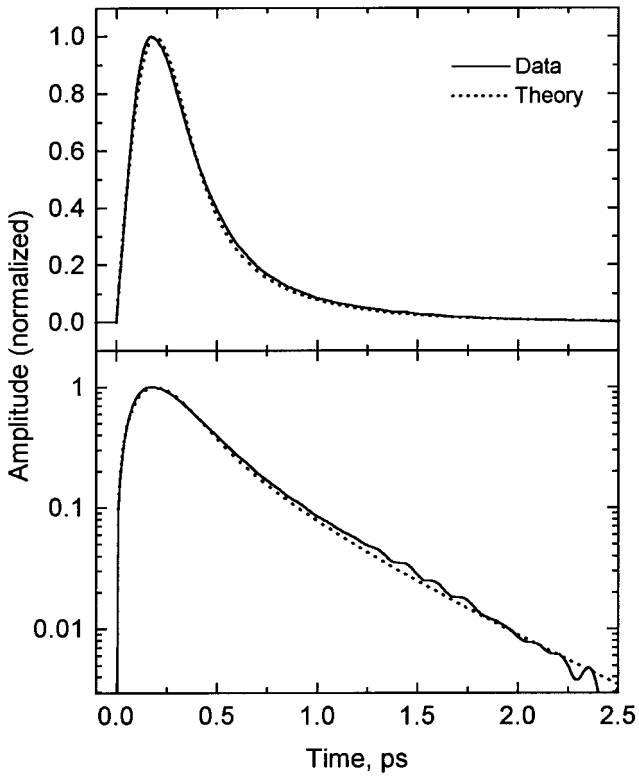

Figure 6. OHD OKE vibrational impulse response function for a 20% solution of CS_2 in *n*-pentane (solid line) is shown together with a fit to the quantum mechanical harmonic-oscillator model (dotted line).

ω_o shifts to lower frequency. A similar saturation effect is observed in the experimental data for CS_2/alkane solutions, as has been noted elsewhere.[31] Thus, although ω_o is expected to continue to decrease as the number density of CS_2 decreases (for a multipolar interaction), both the dynamical waveform and spectral density cease to evolve. This saturation effect is not inconsistent with the interaction model, and is a consequence of the unique frequency relations for intermolecular coordinates at low frequencies that fulfill the relationship $\omega \approx \omega_c \approx \Delta\omega$ noted above.

The quantum oscillator model has been applied to OHD OKE data collected for a series of CS_2 solutions in *n*-pentane. The results of this analysis for the different mixtures are collected in Table 1. Figure 6 shows the vibrational impulse response function for a 20% solution of CS_2 in *n*-pentane, together with a fit to the quantum oscillator model. The quality of the fit in this case is comparable to that of Figure 3 for *neat* CS_2. For each of the solutions investigated, the agreement is quite good, considering the complexity of the waveforms involved and the simplicity of the model (the results of Figure 6 represent the poorest agreement of the data sets analyzed). It is important to note again that the fitted response function represents a single, inhomogeneously broadened harmonic coordinate.

The data of Table 1 reveal that, within the framework of the inhomogeneously broadened quantum harmonic oscillator model, the primary contributor to the dynamical/spectral evolution of the CS_2/alkane data is a shift in the characteristic frequency, ω_o, of the distribution function, $g(\omega)$. Both the width parameter, σ, and the relaxation rate, Γ, remain relatively unchanged through the series. The fitted data of Figures 3 and 6 reveal that the quantum oscillator model for a single nuclear coordinate does an excellent job of accounting for the qualitative trends of the CS_2/*n*-pentane OKE data, and a very good job with the quantitative agreement. We note that the fitting parameters given

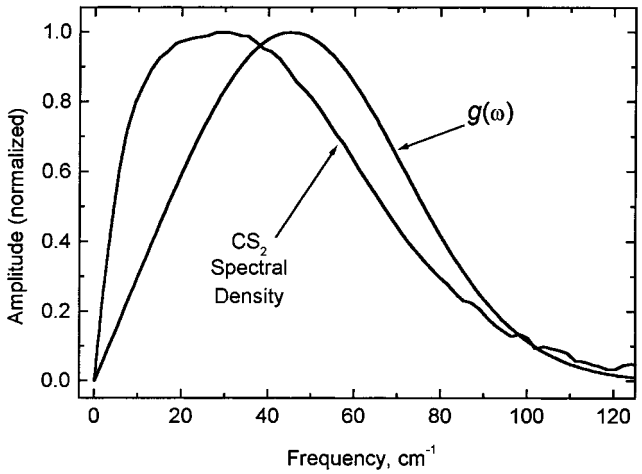

Figure 7. Experimentally measured spectral density function for neat CS_2 compared to the distribution function, $g(\omega)$, determined from the fitting procedure and used to generate the theoretical curve of Figure 3.

in Table 1 are fairly unique (to within the experimental error), such that σ and ω_o cannot be played against one another to obtain equally good agreement, and that the quality of the fit is quite sensitive to variations of the parameters. We also note that the reduced data sets used in this analysis are sensitive to both the quality of the original data and the procedure used for removing the diffusive reorientational contribution. Nevertheless, the ability of the model to account for the trends of the data is impressive. It is interesting to note that while the experimental spectral bandwidth decreases with increasing dilution, the characteristic width parameter, σ, of the quantum HO model remains effectively constant. This is in contrast to the behavior of the classical HO and multimode analyses, in which σ decreases in a monotonic fashion with increasing alkane concentration.[17,27,37] The present result is in agreement with the expectations of reference 31.

Further, we note that the relaxation rate Γ is not equivalent to the $1/e$ time of the exponential tail of the intermolecular response (cf., Figure 1). Within this model, the subpicosecond quasi-exponential decay feature of the intermolecular response in liquids is accounted for without invoking a dynamic process that matches the experimentally observed $1/e$ time constant (the value of the observed $1/e$ decay time of the intermolecular "tail" is approximately one-half of the damping constant $1/\Gamma$ extracted from the analysis). As a result, the common assumption that this time constant directly represents the rate of local structure fluctuations in liquids needs to be reexamined.

It is interesting to compare the experimentally measured spectral density to the distribution function, $g(\omega)$, determined from the fitting procedure. Figure 7 shows the vibrational spectral density function for neat CS_2 (the imaginary part of the Fourier transform of the response function shown in Figure 3), together with the distribution function corresponding to the theoretical curve of Figure 3. The striking difference between the two curves arises from the $1/\omega$ dependence of the response function, eq 18, which leads to a nonlinear weighting of the lowest-frequency contributions to the density of states. Clearly, this effect has a profound impact on the experimental observable.

V. Discussion

The quantum mechanical HO model applied in the previous sections does an excellent job of accounting for both the qualitative and quantitative aspects of the CS_2/alkane OKE data.

The complex dynamical profile (or line shape) associated with the subpicosecond intermolecular dynamics is addressed in a unified manner in terms of a simple functional form. The three-parameter response function provides an excellent account of the complex dynamical profile of *neat* CS_2, as well as the evolution in this dynamical profile as CS_2 is diluted with weakly interacting alkane solvent. The description of the intermolecular dynamics of the highly symmetric CS_2 molecule in terms of *a single vibrational coordinate* is quite appealing, eliminating the need to assign the intermediate-lifetime, quasi-exponential relaxation to a unique nuclear coordinate (as is necessary in multimode curve fitting approaches). For highly symmetric molecular species, such as CS_2, such assignments are questionable, at best.

The present model provides insight into the origin of the complex intermolecular OKE line shape, and suggests that the apparent universality of the quasi-exponential relaxation is a natural consequence of the low-frequency nature of intermolecular vibrational modes in liquids. This signal contribution is expected whenever the oscillator frequency, ω, becomes less than that of the damping/dephasing rate, Γ, as is the usual condition for the intermolecular coordinates of molecular liquids. The present analysis does not, however, address the physical origin of the exponential time constant, which is characterized by the parameter Γ. A recent analysis of temperature-dependent OHD OKE data for a range of symmetric top molecular liquids provides insight into this issue.[30] That work revealed that the exponential relaxation time is highly correlated with the collective orientational correlation time, suggesting that the time constant might be a consequence of spectral diffusion.[30] This hypothesis seems reasonable within the framework of our present understanding of the nature of intermolecular coordinates in liquids. As noted in,[30] however, additional work is required to test this hypothesis.

Recently, Steffen et al.[31] noted some peculiar aspects of the behavior of the CS_2 OKE with respect to dilution in alkane solvents. The two primary observations noted were as follows: (i) very little spectral evolution occurs for CS_2 concentrations below 20 vol % even though, at this concentration, the CS_2 molecules are not yet fully solvated by alkane molecules; and (ii) an apparent decrease in the inhomogeneous spectral width is observed on dilution when, on the basis of entropy considerations, a broadening is expected. Each of these observations is addressed within the framework of the quantum HO models described here. When the unique characteristics of intermolecular degrees of freedom are considered, the observed behavior is in agreement with expectations based on first-order changes in the multipole intermolecular potential, and it is unnecessary to speculate on higher-order effects as the primary cause of the observed spectral evolution.

We return to the issue of the saturation of the spectral shift for CS_2 concentrations of less than 20%, which is addressed above in the discussion of Figures 4 and 5. The behavior of the spectral density and temporal response functions noted there is a consequence of two effects that originate in the equalities of eq 8. The first half of eq 8 relates to the fact that $\omega \approx \Gamma$ for intermolecular oscillators. For constant Γ, as the oscillator shifts to lower frequency ($\omega < \Gamma$), the impulse response function approaches the critically damped limit. In this case eq 18 can be written as

$$\lim_{\omega \to 0} r_n^{(3)}(\omega,t) = r_n^{(3)}(t) = \frac{\alpha_1^2}{2m} t e^{-\Gamma t} \qquad (22)$$

As is evident, in this limit, the impulse response function is independent of frequency and depends exclusively on the dephasing rate, Γ. Thus, to the extent that Γ is constant, all oscillators for which the limiting condition of $\omega \ll \Gamma$ is fulfilled will *exhibit identical OKE response functions*. This limiting case is attained for $\omega \approx \Gamma/4$, but the oscillators begin to take on critically damped character as ω becomes less than Γ.

A second contribution to the saturation effect arises as a consequence of the inhomogeneous character of the intermolecular degrees of freedom, and the near equality of the oscillator frequency and the inhomogeneous width ($\omega \approx \Delta\omega$). This can be addressed within the framework of eq 20. When the characteristic frequency of the distribution, ω_o, and the spectral width, $\Delta\omega$ (which is characterized by the parameter σ), are of the same magnitude the distribution function becomes markedly asymmetric. The precise shape depends on the relative values of the parameters ω_o and σ. This behavior is distinctly different from that of isolated resonances for which ω_o typically is much greater than σ. For the limiting case in which $\omega_o \ll \sigma$, the shape becomes independent of ω_o. Thus, for a fixed value of σ, there will be some value of ω_o below which the distribution will cease to evolve. For the parameters used to generate the data of Figures 4 and 5, the antisymmetric Gaussian distribution function ceases to undergo any significant spectral evolution for $\omega_o < \sigma/2$.

Thus, within the harmonic oscillator model presented here, a saturation in the spectral evolution is expected as the oscillator frequencies become small. Both effects noted here are manifested in the spectral evolution that is evident in the data of Figure 5. Both effects are unique to low-frequency modes, and have no known analogue in the vibrational spectroscopy of high-frequency intramolecular modes.[77] Specifically, the condition $\omega_o < \sigma/2$ is satisfied for solutions of less than approximately 25 vol % CS_2 and appears to be the primary contributor to the spectral saturation in this system. The condition $\omega \leq \Gamma/4$ is fulfilled for lower-frequency oscillators of the distribution at all concentrations, and contributes to the ubiquitous presence of the quasi-exponential relaxation.

The narrowing of the observed intermolecular spectral density of CS_2 on dilution in alkane solvents appears counterintuitive at first glance. Experience with isolated, intramolecular resonances teaches us that, on dilution, line broadening is expected, with the maximum line width typically observed for the 50% solution, reflecting the maximum number of local configurations (maximum entropy). On further dilution, the (shifted) line will narrow as the solute molecules become fully solvated. This line-broadening effect is a consequence of the overlap of two (or more) shifted Raman lines which correspond to differently solvated species in the solution.

The same physical principles apply to the case of intermolecular vibrational modes, with at least two additional constraints, however. Intermolecular modes, like their intramolecular counterparts, can shift either to higher or lower frequency, depending on whether the solute−solvent interaction is stronger or weaker than the solute−solute interaction. They can even remain effectively unshifted, as in the case of benzene/CCl_4 solutions.[67] For the present case, CS_2−CS_2 interactions are mediated by the electrostatic multipole potential.[17,26,27] A substantial contribution to the interactions derive from the large permanent quadrupole moments of the CS_2 molecules.[68] In contrast, the multipole moments of the alkanes are all negligibly small,[23] such that alkane−alkane and CS_2−alkane interactions are small compared to CS_2−CS_2 interactions. It is expected, therefore, that the intermolecular vibrational frequencies will decrease on dilution in alkane solvents.[17,27] An additional constraint that must be recognized for intermolecular vibrational

modes is the zero-frequency "barrier": the oscillator frequencies cannot become negative. More correctly, the low-frequency shape of the spectral density function is determined by the time scale of damping and dephasing processes in the liquid, which is exemplified by Γ in eq 18 and appears to remain largely unchanged[78] through the dilution series.[17,31] On dilution with alkane solvents, as is discussed above, the higher-frequency CS_2 molecular oscillators *must* shift to lower frequency. To the extent that Γ is approximately constant throughout the dilution series, the lower-frequency edge of the spectral line shape remains largely unchanged. The net effect is a compression (narrowing) of the spectral density such that the intermolecular spectrum for CS_2 molecules *completely solvated by alkane species* is compressed toward the low-frequency edge of the intermolecular spectral density of *neat* CS_2. For intermediate concentrations, the vibrational spectrum will lie between these two extremes. Thus, for CS_2/alkane solutions, to the extent that the spectral evolution is determined primarily by changes in the multipolar intermolecular potentials, the OKE spectral density is expected to be *narrower* than that of the *neat* CS_2 solution. The arguments presented here apply to the case of a strongly interacting solute diluted by a weakly interacting solvent. If the roles of the solvent and solute are reversed, the oscillator frequencies will shift higher, and the broadening expected from considerations of intramolecular resonances will be observed. As is evident from a comparison of the data of Figures 1−6 this effect, which might be referred to as the *frequency pile-up effect*, can have a significant impact on the experimental observable.

A central issue, that has been the subject of recent debate,[27,32,33,36,38,39,59] is the degree to which the intermolecular modes in liquids are inhomogeneously broadened. It is widely acknowledged that third-order coherent Raman techniques, such as the optical Kerr effect, cannot directly demonstrate the presence of inhomogeneous broadening in the nuclear coordinates.[45] Line shape analyses that are based on specific models for molecular motion, however, can provide insight into the physical processes relevant to the experimental observables. Such analyses have been utilized for many years, with varying degrees of success, to investigate infrared and Raman vibrational spectra, and more recently for the analysis of stimulated Raman spectrocopies, including the optical Kerr effect. The multimode curve-fitting analyses noted above, which have provided significant insight into the ultrafast dynamics of molecular liquids, fall into this category.

To the extent that the intermolecular vibrational dynamics of liquids can be described in terms of a linearly independent collection of oscillators (harmonic or otherwise), the present results make a strong statement with regard to the question of inhomogeneity in liquids. Within the framework of the quantum oscillator model, the presence of the characteristic temporal signature that is observed for CS_2, solutions of CS_2 with alkane solvents, and numerous other liquids, *is a direct indication that the mode in question is inhomogeneously broadened*.[79] Stated conversely, the characteristic temporal signature of intermolecular modes in liquids, a fast Gaussian-like decay followed by a slower quasi-exponential relaxation, cannot be accounted for in terms of exponentially damped sinusoids without the consideration of inhomogeneous broadening. In view of the quantum HO analysis presented above, the alternate possibilities of two independent modes, or a single homogeneously broadened degree of freedom with the required complex, two-component relaxation dynamics respectively invoke a complexity in the liquid structure that is inconsistent with the symmetry of CS_2, and a response function that cannot be supported by a conventional equation of motion.

It is useful to diverge briefly on this point. The term "inhomogeneous broadening" often connotes a static distribution of molecular environments, as might exist in a glass. Clearly such a condition is inappropriate in liquids. It is more appropriate to refer to a mode as being "inhomogeneously broadened on a given time scale". This is equivalent to stating that, at a given instant in time, there exists a distribution of molecular environments (intermolecular potentials) in the liquid, and that this distribution persists for a finite period of time. For intermolecular modes, the relevant time scale clearly is that of the damping and dephasing (including spectral diffusion[30]) processes that alter the local intermolecular configuration. For most molecular liquids at room temperature, this time scale lies somewhere between 500 fs and 1 ps. The destructive interference effects that result in the rapid Gaussian-like relaxation evident in the OKE of CS_2 and other liquids require that the local structure persist for only a few hundred femtoseconds (the relevant time constant is 160 fs for CS_2 and 80 fs for benzene). Thus, for the effects of inhomogeneous broadening in liquids to be manifested in a femtosecond NLO experiment, it is sufficient that the local structure persist for only a few hundred femtoseconds.

Fifth-order two-dimensional (2-D) Raman experiments hold promise for separating experimentally the homogeneous and inhomogeneous contributions to the intermolecular vibrational line shape.[45,46,70] For the past several years, significant effort has been expended toward developing and interpreting the fifth-order experiment,[32−44] with recent work[41,42] revealing that many of the earlier results were contaminated by cascaded third-order signals that mask the weak fifth-order signals. Recent experiments have been designed to minimize such interfering signal contributions.[43,44] In the fifth-order intermolecular Raman experiment, a pair of time-coincident pulses creates a vibrational coherence; a second pair of pulses, separated from the first by a delay τ_2, alters that coherence in a manner that can initiate a rephasing process that serves to remove the inhomogeneous contribution to the relaxation. The resulting coherence is probed by a fifth pulse (at a delay τ_4 relative to the second pulse pair) in a manner that is analogous to that of third-order experiments. The rephasing is expected to be complete when $\tau_2 = \tau_4$, with the effects of inhomogeneous broadening expected to appear in the 2-D data as signal amplitude along $\tau_2 = \tau_4$ (in the ideal case, for a static distribution, a ridge along $\tau_2 = \tau_4$ is expected).

For the fifth-order experiments reported to date, the 2-D signal decays very rapidly along $\tau_2 = \tau_4$,[43,44] with no evidence for the expected "ridge". Correspondingly, in apparent disagreement with the conclusions based on third-order measurements[16,17,27] and the successes of instantaneous normal mode calculations,[48,49,52,54] the fifth-order measurements suggest that the intermolecular spectrum of CS_2 is well described in terms of homogeneous broadening of the intermolecular vibrational coordinates. Although additional work will be required to fully understand both the third- and fifth-order results to resolve this apparent contradiction, we make a few relevant points here. The lowest-order contribution to the fifth-order response involves the second-derivative term in the polarizability expansion.[25,51,52] Recent work suggests that the fifth-order signal arises largely as a result of collision-induced (dipole−induced dipole) effects, with the contribution from molecular (libration-like) coordinates expected to be negligible.[51,70] In contrast, recent work[52] suggests that the third-order signal for nonassociated liquids (including CS_2) arises predominately from the first-derivative term, and is dominated by molecular contributions.[51] Because the frequency

dependence and damping/dephasing characteristics of molecular and collision-induced contributions to the many-body polarizability tensor are expected to be different, it is not particularly surprising that the two experiments lead to different conclusions regarding the degree of inhomogeneity associated with the intermolecular coordinates.[80] Therefore, rather than concluding that the intermolecular coordinates are homogeneously broadened, it might be more appropriate ask why the inhomogeneous character of molecular liquids is not manifested in the fifth-order experiment. One consideration in this regard is the suppression of the rephasing process through mode coupling.[40] Instantaneous normal mode calculations of the 2-D fifth-order response reveal that nonlinear polarizability coupling between modes (mode mixing) results in a significant suppression of the rephasing process.[40] Further, with the inclusion of vibrational relaxation in the calculations, all evidence for inhomogeneous broadening is eliminated.[40] Although the significance of these results is a subject of current discussion, it is clear that a more complete understanding of the fifth-order results is required before conclusions are made regarding the degree of homogeneity of intermolecular coordinates.

Finally, we address the issue of the coordinate dependence of the molecular polarizability in the third-order experiment. The results presented here illustrate that a response function derived on the basis of a polarizability that is linear in the nuclear coordinates (the Placzek approximation[51]) is sufficient to characterize the third-order nuclear dynamics of CS_2 and its *n*-alkane dilutions. In the most general case, however, higher-order terms can contribute to the polarizability response function. In the circumstance that the coefficient of the quadratic term is nonvanishing, the response function (eqs 16−18) acquires a second (2 "phonon") contribution[37]

$$r_v^{(3)}(\omega,\tau_1) = \frac{\alpha_1^2}{2m\omega} e^{-\Gamma_1\tau_1}\sin(\omega\tau_1) + \frac{\alpha_2^2\hbar}{2m^2\omega^2} \sum_{\lambda}(2\lambda+1)P(\lambda)e^{-\Gamma_2\tau_1}\sin(2\omega\tau_1) \quad (23)$$

where α_2 is defined by the expansion $\alpha(q) = \alpha_1 q + \alpha_2 q^2 + \cdots$. In this case, the spectral density generated by the Fourier transform operations is no longer a linear superposition of single phonon line shapes, and contains an additional two phonon contribution that results from the quadratic dependence of the polarizability on the nuclear coordinate *q*. Therefore, in the general case where the nuclear dependence of the polarizability is unknown, interpretation of the spectral density deduced by data manipulations such as eqs 2 and 3 in terms of a sum of one-phonon vibrational line shapes may be inappropriate. Furthermore, if the polarizability is known to be nonlinear in the nuclear coordinates, data manipulations such as the subtraction of empirically identified response components cannot be identified with removing the contribution of a particular coordinate from the response function of eqs 5 and 6, since individual coordinates may appear in both the linear and nonlinear parts of the nuclear response function. The second term in the response function explicitly includes coupling between nuclear coordinates and a dependence on line broadening mechanisms that is distinct from the linear term.[25]

A response function of the form represented by eq 23 was utilized in the analysis of the third-order response of pure liquid water,[25] where unlike the case of CS_2 and other nonassociated organic molecular liquids in general, the time constant of the longest-lived component of the measured OHD-OKE response did not agree with the reorientation rate extracted from non-optical measurements, an observation that suggests that nonlinear coordinate coupling may be significant.[25] Because the spectral density of the second term is biased to low frequency by the $1/\omega^2$ coefficient, the slow, low-frequency dynamics are expected to be a reasonable diagnostic of the need for the inclusion of nonlinear coordinate terms in the response function. The assumed response function linearity explicit in eqs 6 and 18 is supported by the agreement of the longest-lived component in the CS_2 OHD-OKE response with the DSE behavior of molecular reorientation as measured by nonoptical techniques.

VI. Conclusions

An inhomogeneously broadened quantum-mechanical harmonic oscillator model of intermolecular nuclear coordinates has been applied to the analysis of subpicosecond optical Kerr effect dynamics of neat CS_2 and its binary solutions in alkane solvents. For an inhomogeneously broadened distribution of oscillators, this model predicts naturally the bimodal character of the subpicosecond OKE dynamics, a Gaussian-like ultrafast decay (1/e time $\approx$ 160 fs for CS_2 at 295 K) and a slower, quasi-exponential relaxation (1/e time $\approx$ 450 fs at 295 K), that is universally observed in molecular liquids. Further, the spectral evolution effects that are observed on dilution with weakly interacting alkane solvents (band narrowing and downshift in the peak frequency) are remarkably well accounted for by this simple description.

A particularly satisfying result of this analysis is the ability to accurately represent the complex, apparently multicomponent subpicosecond dynamics with a response function for a single (intermolecular) vibrational coordinate. Analytical descriptions of the bimodal character of the dynamics derived from multimode curve-fitting[16,17,27] require at least two independent intermolecular coordinates. For a rodlike molecule such as CS_2 that decomposition, whether the second coordinate is presumed to be associated with interaction-induced effects, molecular complex formation, or some other interaction, is difficult to justify.

Furthermore, within the quantum mechanical harmonic oscillator representation of the nuclear response functions, inhomogeneous broadening of the nuclear coordinate is required to achieve this result; the presence in the OKE data of the characteristic Gaussian-like ultrafast decay followed by a slower, quasi-exponential relaxation, is a clear indication that the intermolecular dynamics are inhomogeneously broadened. This characterization of the nuclear dynamics does not contravene the theoretical limitations on the information content of third-order nonlinear spectroscopy in the nonresonant regime since it is a model-based result. The advantages of the third-order experiment and the data analysis we have described are their directness, simplicity, and the uniqueness of the physical model for the constraints of the CS_2/dilution system. While the successful implementation of this analysis to CS_2 and its binary solutions in alkanes is possibly a consequence of the simplicity of the intermolecular structure and dynamics of this system, the result remains remarkable due to the simplicity and generality of the model.

It is important to recall that the universal behavior of low frequency intermolecular dynamics in liquids cannot be recovered from the classical oscillator model for the intermolecular coordinates: the mutual pulling of the oscillator damping and frequency results in a continuous loss of oscillator energy to the surrounding solvent bath and a dynamical characteristic that contravenes the experimental observable. Conversely, we have shown that a quantum-mechanical oscillator model, where

stationary energy levels are damped in the weak coupling limit, results in an impressive fit to the experimentally observed dynamics with a minimum of model assumptions and constraints. The details of the physical implications of the distinctions between the classical and quantum representations will be explored in a future report.

In future work, we will extend this analysis to address the temperature-dependent OKE dynamics of CS_2 and acetonitrile liquids, and to systems such as substituted benzenes[56] for which the lower molecular symmetry demands the invocation of more than one intermolecular coordinate. At low temperature the OKE spectral density of molecular liquids develops a pronounced bimodal character,[50] with the high-frequency contributions shifting to higher frequency.[50] In the time domain, the OKE transients develop significantly more pronounced oscillatory character. A preliminary analysis indicates that the quantum oscillator model does a good job of describing the spectra and dynamics, despite the increased complexity of the lower temperature dynamics. In the analysis of temperature-dependent structural dynamics, we will pay particular attention to the treatment of damping, which was limited here to be level independent (but more generally can include level-dependent damping[37,50]). The monosubstituted benzene liquids have been recognized by ourselves[56,60] and others[61] as exhibiting OKE dynamics consistent with multicoordinate (mode) molecular and intermolecular structure. The efficacy of the quantum HO model to yield a unique characterization of the low-frequency nuclear dynamics and spectral density with a multicoordinate system and level-dependent damping will be a valuable test of the limits of this analysis. Finally, we note that recent experimental developments permit complete characterization of the independent third-order nonlinear-optical tensor elements.[71−73] These developments permit independent investigation of the isotropic scattering contributions which, for intermolecular coordinates, arise purely from interaction-induced effects. Analysis of the interaction-induced contributions to the third-order nonlinear-optical response is expected to provide new insights into the nature of the intermolecular coordinates of liquids.

Acknowledgment. The authors acknowledge helpful conversations with John Fourkas. This work was supported by the Office of Naval Research.

Note Added after ASAP Posting. This manuscript was originally published on 7/27/01 with a slight typographical error in eq 17. The corrected version was posted on 7/31/01.

References and Notes

(1) Gordon, R. G. *J. Chem. Phys.* **1965**, *44*, 1307.
(2) Starunov, V. S. *Soviet Phys. Dokl.* **1964**, *8*, 1206. Starunov, V. S. *Opt. Spectrosc.* **1965**, *18*, 165.
(3) McTeague, J. P.; Fleury, P. A.; Dupree, D. B. *Phys. Rev.* **1969**, *188*, 303.
(4) Wang, C. H.; Wright, R. B. *J. Chem. Phys.* **1972**, *55*, 1617.
(5) McDivett, N. T.; Fately, W. G. *J. Mol. Struct.* **1970**, *5*, 477.
(6) Lund, P. A.; Nielsen; O. F.; Praestgaard, E. *Chem. Phys.* **1977**, *28*, 167.
(7) Bucaro, J. A.; Litovitz, T. A. *J. Chem. Phys.* **1971**, *54*, 3846. Dardy, H. D.; Volterra, V.; Litovitz, T. A. *J. Chem. Phys.* **1973**, *59*, 4491.
(8) Alms, B. R.; Bauer, D. R.; Brauman, J. I.; Pecora, R. *J. Chem. Phys.* **1973**, *59*, 5310.
(9) Cox, T. I.; Battaglia, M. R.; Madden, P. A. *Mol. Phys.* **1979**, *38*, 1539.
(10) Kivelson, D.; Madden, P. A. *Annu. Rev. Phys. Chem.* **1980**, *31*, 523.
(11) Moller, K. D.; Rothschild, W. G. *Far-Infrared Spectroscopy*; Wiley-Interscience: New York, 1971.
(12) Perrot, M.; Brooker, M. H.; Lascombe, J. *J. Chem. Phys.* **1981**, *74*, 2787.
(13) Scarparo, M. A. F.; Lee, J. H.; Song, J. *J. Opt. Lett.* **1981**, *34*, 193.
(14) Yarwood, J. in: *Annual Reports on the Progress of Chemistry*; Royal Society of Chemistry, London, 1982; Vol 79, sec. C, pp 157−179.
(15) Kalpouzos, C.; McMorrow, D.; Lotshaw, W. T.; Kenney-Wallace, G. A. *J. Phys. Chem.* **1987**, *91*, 2028.
(16) McMorrow, D.; Lotshaw, W. T.; Kenney-Wallace, G. A. *IEEE J. Quantum Elect.* **1988**, QE−24, 443.
(17) Kalpouzos, C.; McMorrow, D.; Lotshaw, W. T.; Kenney-Wallace, G. A. *Chem. Phys. Lett.* **1988**, *150*, 138, Kalpouzos, C.; McMorrow, D.; Lotshaw, W. T.; Kenney-Wallace, G. A. *Chem. Phys. Lett.* **1989**, *155*, 240.
(18) McMorrow, D.; Lotshaw, W. T. *Chem. Phys. Lett.* **1990**, *174*, 85. McMorrow, E. *Opt. Comm.* **1990**, *86*, 236.
(19) Hattori, T.; Kobayashi, T. *J. Chem. Phys.* **1991**, *24*, 3332.
(20) Ruhman, S.; Nelson, K. A. *J. Chem. Phys.* **1991**, *94*, 859.
(21) Chang, Y. J.; Castner, E. W., Jr. *J. Chem. Phys.* **1993**, *99*, 113.
(22) Chang,Y. J.; Castner, E. W., Jr. *J. Chem. Phys.* **1993**, *99*, 7289.
(23) Chang, Y. J.; Castner, E. W., Jr. *J. Phys. Chem.* **1996**, *100*, 3330.
(24) Cho, M.; Du, M.; Scherer, N. F.; Fleming, G. R.; Mukamel, S. *J. Chem. Phys.* **1993**, *99*, 2410.
(25) Palese, S.; Mukamel, S.; Miller, R. J. D.; Lotshaw, W. T. *J. Phys. Chem.* **1996**, *100*, 10 380.
(26) Lotshaw, W. T.; McMorrow, D.; Thantu, N.; Melinger, J. S.; Kitchenham, R. *J. Ram. Spectrosc.* **1995**, *26*, 571.
(27) McMorrow, D.; Thantu, N.; Melinger, J. S.; Kim, S.; Lotshaw, W. T. *J. Phys. Chem.* **1996**, *100*, 10389.
(28) Quitevis, E. L.; Neelakandan, M. *J. Phys. Chem.* **1996**, *100*, 10 006.
(29) Neelakandan, M.; Pant, D.; Quitevis, E. L. *J. Phys. Chem.* **1997**, *101*, 2936.
(30) Loughnane, B. J.; Scodinu, A.; Farrer, R. A.; Fourkas, J. T. *J. Chem. Phys.* **1999**, *111*, 2686.
(31) Steffen, T.; Meinders, N. A. C.; Duppen, K. *J. Phys. Chem.* **1998**, *102*, 4213.
(32) Tominaga, K.; Naitoh, Y.; Kang, T. J.; Yoshihara, K. in Ultrafast Phenomena IX, Springer, Berlin, 1994; pp 143−144. Tominaga, K.; Yoshihara, K. *Phys. Rev. Lett.* **1995**, *74*, 3061.
(33) Tominaga, K.; Keogh, G. P.; Naitoh, Y.; Yoshihara, K. *J. Ram. Spectrosc.* **1995**, *26*, 495.
(34) Tominaga, K.; Yoshihara, K. *J. Chem. Phys.* **1996**, *104*, 1159.
(35) Tominaga, K.; Yoshihara, K. *J. Chem. Phys.* **1996**, *104*, 4419.
(36) Steffen, T.; Duppen, K. *Phys. Rev. Lett.* **1996**, *76*, 1224.
(37) Steffen, T.; Fourkas, J. T.; Duppen, K. *J. Chem. Phys.* **1996**, *105*, 7364. Steffen, T.; Duppen, K. *J. Chem. Phys.* **1996**, *106*, 3854.
(38) Tokmakoff, A.; Fleming, G. R. *J. Chem. Phys.* **1997**, *106*, 2569.
(39) Tokmakoff, A.; Lang, M. J.; Jordanides, X. J.; Fleming, G. R. *Chem. Phys.* **1998**, *233*, 231.
(40) Saito, S.; Ohmine, I. *J. Chem. Phys.* **1998**, *108*, 240.
(41) Ulness, D. J.; Kirkwood, J. C.; Albrecht, A. C. *J. Chem. Phys.* **1998**, *108*, 3897.
(42) Blank, D. A.; Kaufman, L. J.; Fleming, G. R. *J. Chem. Phys.* **1999**, *111*, 3105.
(43) Blank, D. A.; Kaufman, L. J.; Fleming, G. R. *J. Chem. Phys.* **2000**, *113*, 771.
(44) Golonzka, O.; Demirdoven, N.; Khalil, M.; Tokmakoff, A. *J. Chem. Phys.* **2000**, *113*, 9893.
(45) Tanimura, Y.; Mukamel, S. *J. Chem. Phys.* **1993**, *99*, 9496.
(46) Mukamel, S. *Principles of Nonlinear Optical Spectroscopy*; Oxford University Press: New York, 1995.
(47) Moore, P.; Keys, T. *J. Chem. Phys.* **1994**, *100*, 7609.
(48) Buchner, M.; Ladanyi, B. M.; Stratt, R. M. *J. Chem. Phys.* **1992**, *97*, 8522.
(49) Ladanyi, B. M.; Stratt, R. M. *J. Chem. Phys.* **1995**, *99*, 2502.
(50) Farrer, R. A.; Loughnane, B. J.; Deschenes, L. A.; Fourkas, J. T. *J. Chem. Phys.* **1997**, *106*, 6901.
(51) Murry, R. L.; Fourkas, J. T. *J. Chem. Phys.* **1997**, *107*, 9726.
(52) Murry, R. L.; Fourkas, J. T.; Keyes, T. *J. Chem. Phys.* **1998**, *109*, 2814.
(53) David, E. F.; Stratt, R. M. *J. Chem. Phys.* **1998**, *109*, 1375.
(54) Ratajska-Gadomska, B.; Gadomski, W.; Wiewior, P.; Radzewicz, C. *J. Chem. Phys.* **1998**, *108*, 8489.
(55) Lotshaw, W. T.; McMorrow, D.; Kalpouzos, C.; Kenney-Wallace, G. A. *Chem. Phys. Lett.* **1987**, *136*, 323.
(56) Lotshaw, W. T.; McMorrow, D.; Kenney-Wallace, G. A. *Proc. SPIE*, **1988**, *981*, 20.
(57) Deeg, F. W.; Stankus, J. J.; Greenfield, S. R.; Newell, V. J.; Fayer, M. D. *J. Chem. Phys.* **1989**, *90*, 6893.
(58) McMorrow, D.; Lotshaw, W. T. *J. Phys. Chem.* **1991**, *95*, 10395.
(59) McMorrow, D.; Lotshaw, W. T. *Chem. Phys. Lett.* **1991**, *178*, 69.
(60) McMorrow, D.; Melinger, J. S.; Lotshaw, W. T. *Quantum Electronics and Laser Science Conference, 1993 OSA Technical Digest Series*, Vol. 12, Optical Society of America, Washington, DC, 1993; pp 84−85.
(61) Friedman, J. S.; She, C. Y. *J. Chem. Phys.* **1993**, *99*, 4960.

(62) McMorrow, D.; Kim, S. K.; Melinger, J. S.; Lotshaw, W. T. in *Ultrafast Phenomena VIII*; Springer: Berlin, 1992; pp 656−657.

(63) Madden, P. A. in *Ultrafast Phenomena IV*; Springer: Berlin, 1984; pp. 224−251.

(64) Berne, B. J.; Pecora, R. *Dynamic Light Scattering*; Wiley: New York, 1976.

(65) Hellwarth, R. W. *Prog. Quantum Elect.* **1977**, *5*, 1.

(66) Kubo, R. in: *Fluctuations, Relaxation, and Resonance in Magnetic Systems*; Har, D. ter., Ed.; Plenum Press: New York, 1962; pp 23−68.

(67) Lotshaw, W. T.; Staver, P. R.; McMorrow, D.; Thantu, N.; Melinger, J. S. in *Ultrafast Phenomena IX*; Springer: Berlin, 1994; pp. 91−92.

(68) Reynolds, L.; Gardecki, J. A.; Frankland, S. J. V.; Horng, M. L.; Maroncelli, M. *J. Phys. Chem.* **1996**, *100*, 10 337.

(69) Fourkas, J. T., private communication.

(70) Fourkas, J. T. In *Advances in Chemical Physics*; Prigogine and Rice, Eds.; Wiley: New York, 2001; Vol. 117, in press.

(71) Goodno, G. D.; Dudusc, G.; Miller, R. J. D. *J. Opt. Soc. Am. B*, **1998**, *15*, 1791.

(72) Khalil, M.; Golonzka, O.; Demirdoven, N.; Fecko, C. J.; Tokmakoff, A. *Chem. Phys. Lett.* **2000**, *321*, 231.

(73) Khalil, M.; Demirdoven, N.; Golonzka, O.; Fecko, C. J.; Tokmakoff, A. *J. Phys. Chem.* **2000**, *104*, 5711.

(74) More distinct oscillations are observed in other liquids at room temperature, including benzene,[16] pyridine,[18] iodobenzene,[18,56] and acetonitrile,[58] with the negative-going feature in the CS_2 data becoming pronounced at lower temperatures.[20]

(75) For C_{2v} molecular species five distinct contributions (time scales) have been identified,[56,60] with additional contributions expected for lower symmetry species.[64]

(76) If appropriate adjustments are made to account for the unique characteristics of low-frequency intermolecular vibrational distrubutions.

(77) Although it is expected that analogous behavior may be present in very low frequency intramolecular modes, such as torsional modes in large molecules.

(78) Although there is some evidence that the decay time for the quasi-exponential component decreases slightly through the dilution series.[69]

(79) This conclusion has been suggested previously in the context of the classical oscillator model.[27,59]

(80) This assertion is supported by the recognition that the results of third-order analyses should not be used unilaterally to simulate fifth-order experimental observables.[25,51]